1521-0103/376/1/29–39$35.00
THE JOURNAL OF PHARMACOLOGY AND EXPERIMENTAL THERAPEUTICS

https://doi.org/10.1124/jpet.120.000291
J Pharmacol Exp Ther 376:29–39, January 2021

Transporter Activity Changes in Nonalcoholic Steatohepatitis: Assessment with Plasma Coproporphyrin I and III[S]

Sagnik Chatterjee,[1] Sambuddho Mukherjee,[1] L.V.J. Sankara Sivaprasad, Tanvi Naik, Shashyendra Singh Gautam, Bokka Venkata Murali, Avinash Annasao Hadambar, Gowtham Raj Gunti, Vijaykumar Kuchibhotla, Avisek Deyati, Sushma Basavanthappa, Manjunath Ramarao, T. Thanga Mariappan, Bradley A. Zinker, Yueping Zhang, Michael Sinz, and Hong Shen

Pharmaceutical Candidate Optimization (S.C., S.S.L.V.J., T.N., S.S.G., B.V.M.) and Discovery and Translational Medicine (S.M., A.A.H., G.R.G., V.K., A.D., S.B.), Biocon Bristol-Myers Squibb R&D Center (BBRC), Syngene International Ltd., Bangalore, India; Pharmaceutical Candidate Optimization (T.T.M.) and Discovery and Translational Medicine, Bristol-Myers Squibb India Pvt. Ltd. (M.R.), Biocon Bristol-Myers Squibb R&D Center (BBRC), Bangalore, India; BMS Fibrosis Drug Discovery, Research and Early Development, Princeton, New Jersey (B.A.Z.); and Pharmaceutical Candidate Optimization, Bristol-Myers Squibb Co., Princeton, New Jersey (Y.Z., M.S., H.S.)

Received August 18, 2020; accepted October 13, 2020

ABSTRACT

Expression and functional changes in the organic anion transporting polypeptide (OATP)–multidrug resistance–associated protein (MRP) axis of transporters are well reported in patients with nonalcoholic steatohepatitis (NASH). These changes can impact plasma and tissue disposition of endo- and exogenous compounds. The transporter alterations are often assessed by administration of a xenobiotic or by transporter proteomic analysis from liver biopsies. Using gene expression, proteomics, and endogenous biomarkers, we show that the gene expression and activity of OATP and MRP transporters are associated with disease progression and recovery in humans and in preclinical animal models of NASH. Decreased OATP and increased MRP3/4 gene expression in two cohorts of patients with steatosis and NASH, as well as gene and protein expression in multiple NASH rodent models, have been established. Coproporphyrin I and III (CP I and III) were established as substrates of MRP4. CP I plasma concentration increased significantly in four animal models of NASH, indicating the transporter changes. Up to a 60-fold increase in CP I plasma concentration was observed in the mouse bile duct–ligated model compared with sham controls. In the choline-deficient amino acid–defined high-fat diet (CDAHFD) model, CP I plasma concentrations increased by >3-fold compared with chow diet–fed mice. In contrast, CP III plasma concentrations remain unaltered in the CDAHFD model, although they increased in the other three NASH models. These results suggest that tracking CP I plasma concentrations can provide transporter modulation information at a functional level in NASH animal models and in patients.

SIGNIFICANCE STATEMENT

Our analysis demonstrates that multidrug resistance–associated protein 4 (MRP4) transporter gene expression tracks with nonalcoholic steatohepatitis (NASH) progression and intervention in patients. Additionally, we show that coproporphyrin I and III (CP I and III) are substrates of MRP4. CP I plasma and liver concentrations increase in different diet- and surgery-induced rodent NASH models, likely explained by both gene- and protein-level changes in transporters. CP I and III are therefore potential plasma-based biomarkers that can track NASH progression in preclinical models and in humans.

Introduction

Nonalcoholic fatty liver disease (NAFLD) and nonalcoholic steatohepatitis (NASH) are global health concerns. NAFLD and progressive forms are commonly associated with lifestyle/dietary irregularities, high cholesterol, obesity, and type 2 diabetes. This spectrum of syndromes is characterized by accumulation of more than 5% fat in liver leading to hepatic steatosis (Chalasani et al., 2018). In a fraction of cases, often accompanied by inflammatory insults, hepatic steatosis can progress to NASH, a more severe form of liver disease with tissue fibrosis (Brunt et al., 2015).

It is reported that expression and function of drug transporters and drug metabolizing enzymes change during NASH.

This study is supported by Bristol Myers Squibb Company.
[1]S.C. and S.M. contributed equally as first author.
https://doi.org/10.1124/jpet.120.000291.
[S] This article has supplemental material available at jpet.aspetjournals.org.

ABBREVIATIONS: ABC, ATP-binding cassette; BDL, bile duct ligation; BNZ, benzbromarone; CDAHFD, choline-deficient amino acid–defined high-fat diet; CP I/III, coproporphyrin I/III; GEO, Gene Expression Omnibus; LC-MS/MS, liquid chromatography–tandem mass spectrometry; MEB, ^{99m}Tc-mebrofrenin; MP, methapyrilene hydrochloride; MRP, multidrug resistance–associated protein; NAFLD, nonalcoholic fatty liver disease; NASH, nonalcoholic steatohepatitis; OATP, organic anion transporting polypeptide; PBPK, physiologically based pharmacokinetic; qPCR, quantitative polymerase chain reaction; SLCO, solute linked carrier organic anion.

The hepatic uptake transporters [organic anion transporting polypeptide (OATP) 1B1 and OATP1B3] are downregulated, basolateral efflux transporters [multidrug resistance–associated protein (MRP) 3 and MRP4] are upregulated, and canalicular efflux transporter (MRP2) is mislocalized (Thakkar et al., 2017; Evers et al., 2018). Two mechanisms are associated with the expression alterations: 1) inflammatory cytokines released during progression of NASH (e.g., Tumour Necrosis Factor alpha, or Interlukin - 6) interact with nuclear receptors such as constitutive androstane receptor (CAR), pregnane X receptor (PXR), farnesoid X receptor (FXR), or liver X receptor (LXR) (Cobbina, and Akhlaghi, 2017), or 2) accumulated bile acids activate FXR (Lin and Kohli, 2018). Post-transcriptional modifications are associated with mislocalization and functional aberration of OATP and MRP2 transporter proteins during NASH (Clarke et al., 2017).

Plasma and hepatic concentrations of drugs that are substrates of OATP-MRP transporters are reported to increase due to these transporter alterations (Ali et al., 2017). Increased hepatic concentrations are reported for the diagnostic agent ^{99m}Tc-mebrofrenin (MEB) in patients with NASH (Ali et al., 2017). Increased plasma concentrations are also reported for pravastatin, simvastatin acid, ezetimibe, and morphine glucuronides in different rodent models of NASH (Lickteig et al., 2007; Clarke et al., 2014a,b, 2015; Hardwick et al., 2014; Dzierlenga et al., 2015; Laho et al., 2016; Suga et al., 2019). These pharmacokinetic alterations can potentially impact safety and efficacy of drugs in patient populations at different stages of disease. Hence, there is a need to understand the exposure changes in diverse populations of patients with NASH compared with healthy volunteers.

An endogenous compound that is a substrate of all the major hepatic drug transporters undergoing significant change in NASH (OATP1B1, OATP1B3, MRP2, MRP3, and MRP4) can provide functional level information about these transporters. Measuring plasma concentrations of an endogenous compound can avoid complications of linking mRNA or protein levels to functional activity. An endogenous plasma-based marker will therefore allow tracking of individual patients in terms of transporter function at particular NASH stages and indicate disease progression.

Coproporphyrin I and III (CP I and III) are byproducts of heme biosynthesis. About 80% of CP biosynthesis takes place in erythrocytes (Wang et al., 2018). Elimination of CPs is completely transporter-mediated, primarily to urine and bile. They are known endogenous biomarkers for predicting OATP1B [solute linked carrier organic anion (*SLCO*) 1B] inhibition-based drug-drug interactions (Lai et al., 2016; Shen et al., 2016). CP I concentrations have been recently used to monitor OATP1B activity in patients with end stage renal disease and recovery after kidney transplantation (Suzuki et al., 2019). In addition to OATP1B, we have shown that CP I is a substrate of MRP2 (Gilibili et al., 2017). MRP2-mediated biliary clearance is compromised in Dubin Johnson syndrome. The increase in renal clearance of CP I and III suggests an involvement of hepatic basolateral efflux transporters to reroute clearance from biliary to renal side in patients with Dubin Johnson syndrome. A previous study indicated CP I and III as substrates of MRP3 [ATP-binding cassette (*ABC*) *C3*], but not MRP4 (*ABCC4*) (Kunze et al., 2018). As CP I and III are known substrates for MRP2/3, and because MRP4 generally shares overlapping substrate specificity with MRP2/3, we reevaluated the substrate potential of CP I and III toward MRP3 and 4 with a modified, highly sensitive method.

The aims of the current studies are to 1) examine the changes in gene and protein expression of major hepatobiliary transporters in patients with NASH and rodent models of NASH and 2) evaluate the effect of altered gene and protein expression of hepatobiliary transporters on plasma and liver concentrations of CP I and III, endogenous biomarkers of OATPs/MRPs in NASH animal models.

Materials and Methods

Chemicals and Reagents. CP I and CP III were purchased from Santa Cruz Biotechnology, Inc. (Dallas, TX). CP I-$^{15}N_4$ sodium bisulfate salt was purchased from Toronto Research Chemicals Inc. (ON, Canada). Ethylacetate (AR grade) was purchased from Spectrochem Pvt. Ltd. (Mumbai, India). Human MRP3- and MEP4-expressing inside-out membrane vesicles (protein concentration 5 mg/ml) derived from Sf9 insect cells were purchased from GenoMembrane, Co., Ltd. (Yokohama, Japan). Reaction incubation plates (96 well, ultralow attachment, polystyrene, flat bottom, clear) were purchased from Corning Costar (NY). Assay plates (96 well, black polystyrene) were used for fluorescence measurement. All standard chemicals for vesicle assays were obtained from Sigma Aldrich (Bangalore, India).

Transcriptomic Analysis of Canadian and French-Belgian Cohorts. We used gene expression data sets with adequate clinical annotation from Canadian [Gene Expression Omnibus (GEO) identifier: GSE89632] and French-Belgian (GEO identifier: GSE83452) cohorts of human patients with NASH from the GEO. Downloaded data sets were normalized in R Studio pipelines. Log2 normalized expression profiles of transporters (i.e., *ABCC2*, *ABCC4*, *ABCC3*, *SLCO1B1*, *SLCO1B3*) within the Canadian cohort were plotted as healthy control, steatosis, and NASH. The French-Belgian cohort was a longitudinal study with 1-year follow-up for a subset of patients. Expression of these transporters was plotted for a subset of patients from the French-Belgian cohort who were initially classified as NASH, with clinical resolution at 1 year after intervention with dietary restriction/bariatric surgery. The presence of NASH was defined according to NASH Clinical Research Network guidelines, assessing combined presence of steatosis, ballooning, and lobular inflammation (Chalasani et al., 2018).

Vesicular Transport Assay. The active uptake of CP I and CP III was assessed using inside-out Sf9 insect cell–derived vesicles overexpressing MRP3 or MRP4. The assay was conducted following methods standardized in house for MRP2 vesicles (Gilibili et al., 2017). Briefly, the vesicle protein (0.2 mg/ml) was incubated for 20 minutes with either CP I (2 μM) or CP III (2 μM) in the presence or absence of inhibitors [100 μM MK-571 or 100 μM benzbromarone (BNZ)] followed by vacuum filtration. CP I and III were analyzed using a fluorimeter (Perkin Elmer Envision). Concentration-dependent transport of CP I and III was assessed using optimized conditions for human MRP3 and 4 and rat Mrp4 vesicles.

Animals. All animal experiments were performed in accordance with protocols approved by the respective Institutional Animal Ethical Committees. Male C57Bl/6 mice and male Sprague-Dawley rats were sourced as indicated. Animals were maintained in ventilated cages at 21–23°C with a 12-hour light/dark cycle and food and water ad libitum. Experimental procedures were conducted in accordance with procedures set by the Committee for the Purpose of Control and Supervision of Experiments on Animals, Government of India.

Bile Duct Ligation Model in Mice and Rats. Adult male C57Bl/6 mice (Envigo, Netherlands) 9 to 10 weeks old and Sprague-Dawley rats (~8 weeks, 260–280 g body weight, Taconic) were used in the studies. All animals were divided into bile duct–ligated and sham control groups [n = 3 per group for rats; n = 6 mice in the sham control group and n = 12 mice in the mouse bile duct ligation (BDL) group]. Cholestatic liver injury was induced by ligating the common bile duct

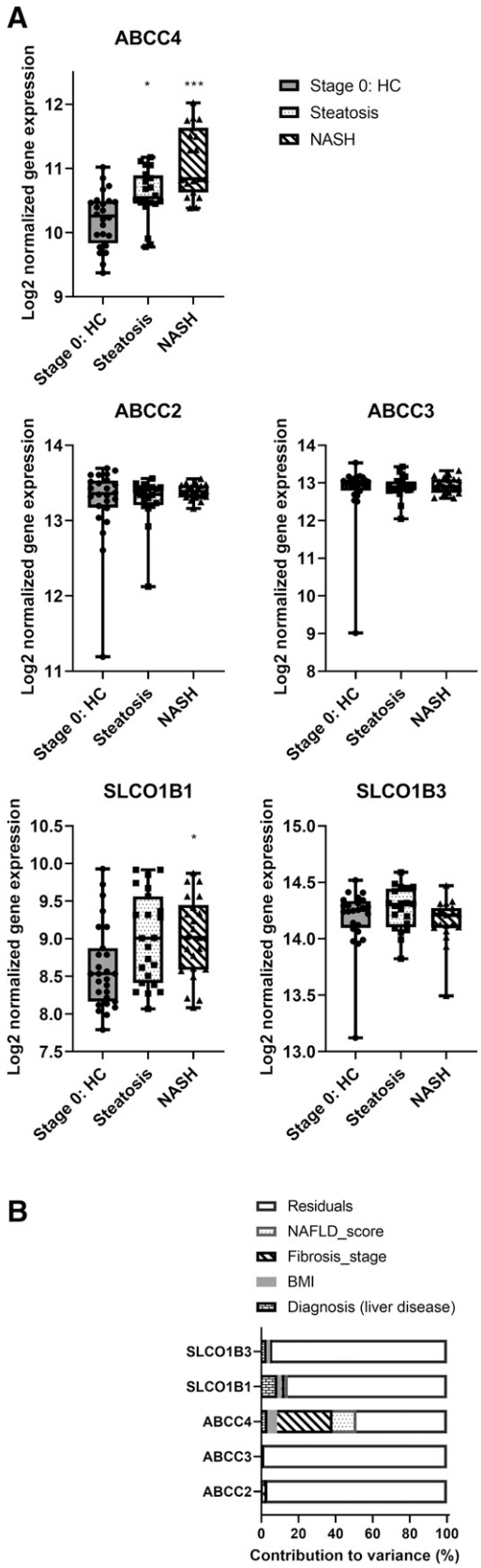

Fig. 1. Global gene expression profile analysis of Canadian NAFLD/NASH cohorts. The Canadian cohort includes clinically staged samples encompassing healthy controls (Stage 0: HC), NAFLD, and NASH. In (A and B), 200 ng quality checked (Agilent BioAnalyzer) RNA from these annotated samples was labeled and amplified after Illumina Whole Genome Expression DASL assay kit and subjected to global expression profiling as indicated with GEO identifier GSE89632. In (B), annotated clinical covariates were compared with transporter expression levels. Further analysis and statistical evaluation were performed as described in *Materials and Methods*. ***$P < 0.001$; *$P < 0.05$. BMI: Body Mass Index

in mice (Tag et al., 2015) and rats (Takita et al., 1988; Yang et al., 2015). To evaluate the time course of changes in expression of transporters and CPs, blood and liver tissues were collected on day 0 (presurgery) and on 1, 3, 5, 7, and 14 days postsurgery in rats. In mice, blood and liver tissue samples were collected on day 0 (before surgery) and on day 10. Blood (200 μl from rat and 100 μl from mice) was collected from each animal and centrifuged at 10,621*g* for 3 minutes at 4°C. The resultant plasma was separated and stored in dark sample collection plates at −80°C. A subset of three rats from both bile duct–ligated and sham control groups were euthanized on days 3, 7, and 14 after the plasma collection. Rat and mouse livers were collected, weighed, and stored at −80°C for further analysis.

Rat Methapyrilene-Induced Model of Cholestatic Liver Injury. Male Sprague-Dawley rats (8 to 9 weeks, Taconic) were administered methapyrilene hydrochloride (MP) at a dose of 150 mg/kg body weight in phosphate-buffered saline by oral gavage three times per week as described (Probert et al., 2014). Rats were euthanized at 3 and 6 weeks of treatment followed by blood and liver collection for biochemical analyses and CP quantitation.

Mouse NASH Model: Choline-Deficient Amino Acid–Defined High-Fat Diet. Single housed C57BL/6J mice (6 weeks; Jackson Laboratories, Bar Harbor, ME) were acclimated for 1 week on standard rodent chow (Teklad 2018, Madison, WI), followed by specialized diets (A06071302; Research Diets, New Brunswick, NJ). After 8, 18, or 22 weeks [22 weeks with choline-deficient amino acid–defined high-fat diet (CDAHFD) only] on diet, mice (n = 5 per time point) were sacrificed at time points indicated from the control and CDAHFD diet groups, and blood samples were collected. The blood samples were centrifuged at 4°C at 1500–2000*g*; plasma was removed and stored at −80°C for later processing.

Sample Collection, RNA Isolation, and Quantitative Polymerase Chain Reaction Assay. Rat, and mouse liver samples (BDL and methapyrilene studies) were collected in RNA Later (Invitrogen, Thermo-Fisher). Tissue lysis was done in Qiazol using Tissue Lyser II (Qiagen). RNA was isolated through MN Nucleospin96 high-throughput vacuum manifold, and concentrations were established using a Thermo NanoDrop8000 Spectrophotometer. Quantitative polymerase chain reaction (qPCR) was performed for all samples in the panel of transporters depicted in Fig. 3, A and B. cDNA synthesis was done using 1000 ng of RNA as input from all samples using iScript RT Supermix as per manufacturer instructions. qPCR was set using SsoFast EvaGreen Supermix (BioRad) in 384-well format on a CFX384 instrument. For data analysis, ddCt with reference to housekeeping marker (peptidyl-prolyl cis-trans isomerase A, *PPIA*) was calculated for each marker, and fold change for BDL samples was normalized with respect to the sham control group.

Membrane Protein Isolation and Trypsin Digestion Procedure. Liver (200 mg) from both sham and BDL rats was subjected to membrane fraction isolation procedure using the ProteoExtract Native Membrane Protein Extraction Kit from Calbiochem (CA), as per manufacturer's protocol (Sun et al., 2005). After trypsin digestion, peptides were subjected to mass spectrometric analysis. The procedures for membrane extraction, trypsin digestion, and instrumentation are detailed in the Supplemental Information. Selection of unique peptides was done as previously described (Gautam et al., 2019) and in the Supplemental Information.

Instrumentation and Chromatographic Conditions for Transporter Protein Quantitation. Waters Acquity Ultraperformance Liquid Chromatography Integrated System (Milford) was used to inject 10 μl aliquots of the processed samples on a reverse-phase column (BEH C18,

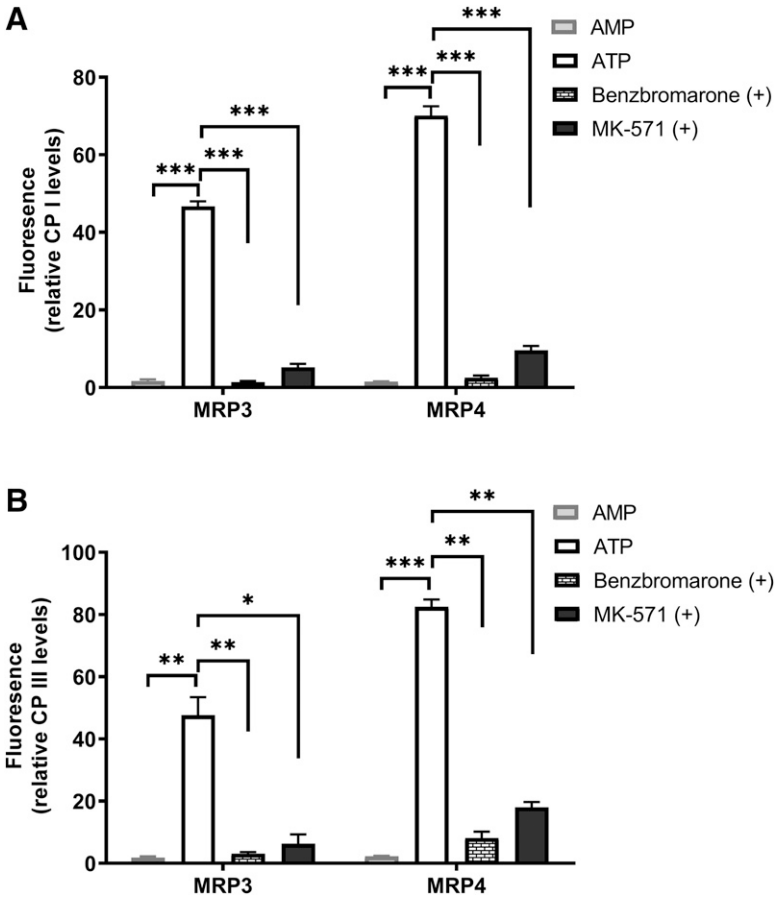

Fig. 2. CP I (A) and III (B) transport in MRP3 and 4 overexpressed membrane vesicles in the presence and absence of inhibitors (MK-571 and benzbromarone). Fluorescence intensity as an average from three wells were plotted for each condition. ***$P < 0.001$; **$P < 0.01$.

1.7 μm, 2.1 × 50 mm; Waters, Milford, MA) maintained at 40 ± 2°C. The liquid chromatography details can be obtained in the Supplemental Information. The analytical data were processed by Analyst software (version 1.6.4). The optimized transitions are provided in Table 1.

The standard calibration curves using synthetic unlabeled peptides from New England Peptides (Boston) were prepared in the range of 0.5 nM–1 μM in bovine serum albumin (0.1% in phosphate-buffered saline). Sample preparation was as described for trypsin digestion procedure except for addition of labeled internal standards for each transporter protein. These peptides were added to 10% v/v formic acid and used during quenching of the tryptic digestion.

Liquid Chromatography–Tandem Mass Spectrometry Method for Quantification of CP I and CP III. Liquid chromatography–tandem mass spectrometry (LC-MS/MS)–based quantification of CP I and CP III from mouse and rat plasma and liver samples used a Acquity UHPLC (Waters Corporation) coupled with a AB Sciex 5500 Q-trap triple quadrupole mass spectrometer (AB Sciex, Framingham, MA), fitted with an electrospray source in positive ionization mode. A labeled internal standard (Coproporphyrin I-15N4) was used for sample quantitation. The isomers of CP were baseline separated using an Ace Excel2 C18 column (150 × 2.1 mm) (Advanced Chromatography Technologies Ltd., Aberdeen, Scotland) and binary gradient elution comprising Mill-Q water with 0.1% formic acid (solvent-A) and acetonitrile with 0.1% formic acid (solvent-B). The following mass spectrometric conditions were used during the analysis: Multiple reaction monitoring (MRM) transitions CP I (655.5→596.3), CP III (655.5→596.3), and d4–CP I (659.3→600.3); capillary voltage, 5500 V; nebulizer and drying gas (high-purity nitrogen) 50 psi; and drying gas temperature 550°C.

Twelve working solutions of CP I and CP III (mixture of CP I and III) were prepared in DMSO. The calibration standards (0.02–1000 nM) were then prepared by spiking respective working solutions in 1% bovine serum albumin (surrogate matrix). Aliquots of 50 μl from each calibration standard and plasma study samples were placed into Eppendorf tubes, along with 20 μl of internal standard ($^{15}N_4$–CP I) and 600 μl of ethyl acetate, vortexed for 2 minutes, and centrifuged for 10 minutes at 14,000*g*. A supernatant of 400 μl was separated from each tube and dried in a nitrogen evaporator set at 40°C until complete dryness. Then the tubes were reconstituted with 150 μl of methanol: water, 70:30%, v/v. The samples were transferred to a 96-well plate and 4 μl was injected on LC-MS/MS. Analyst version 1.6.2 was used for system control and data processing.

Statistical Analyses. Gene expression microarray data sets from both French Belgian and Canadian cohorts were normalized with Robust Multi-Array Average Expression Measure, a function from the affy package (version 1.50.0) in R statistical software (version 4.0.2). Normalized data sets were then imported to GraphPad Prism to estimate statistical significance of transporters expression difference across three groups in the Canadian cohort (Brown-Forsythe and Welch's ANOVA tests with residual plots to account for independent variables). For all data sets with only two conditions, an unpaired *t* test (assuming Gaussian distribution) with Welch's correction was performed. The contribution of different clinical covariates to gene expression of these transporters was calculated using variancePartition package (version 1.18.3) in R (version 4.0.2), which implemented a linear mixed model to calculate variance contributed by each clinical covariate.

Results

Hepatobiliary Transporter Expression in Patients with NASH. We evaluated the gene expression of key liver transporters in two distinct publicly available, clinically annotated cohorts of patients with NASH. Global expression profiling in the Canadian cohort included healthy controls ($n = 24$),

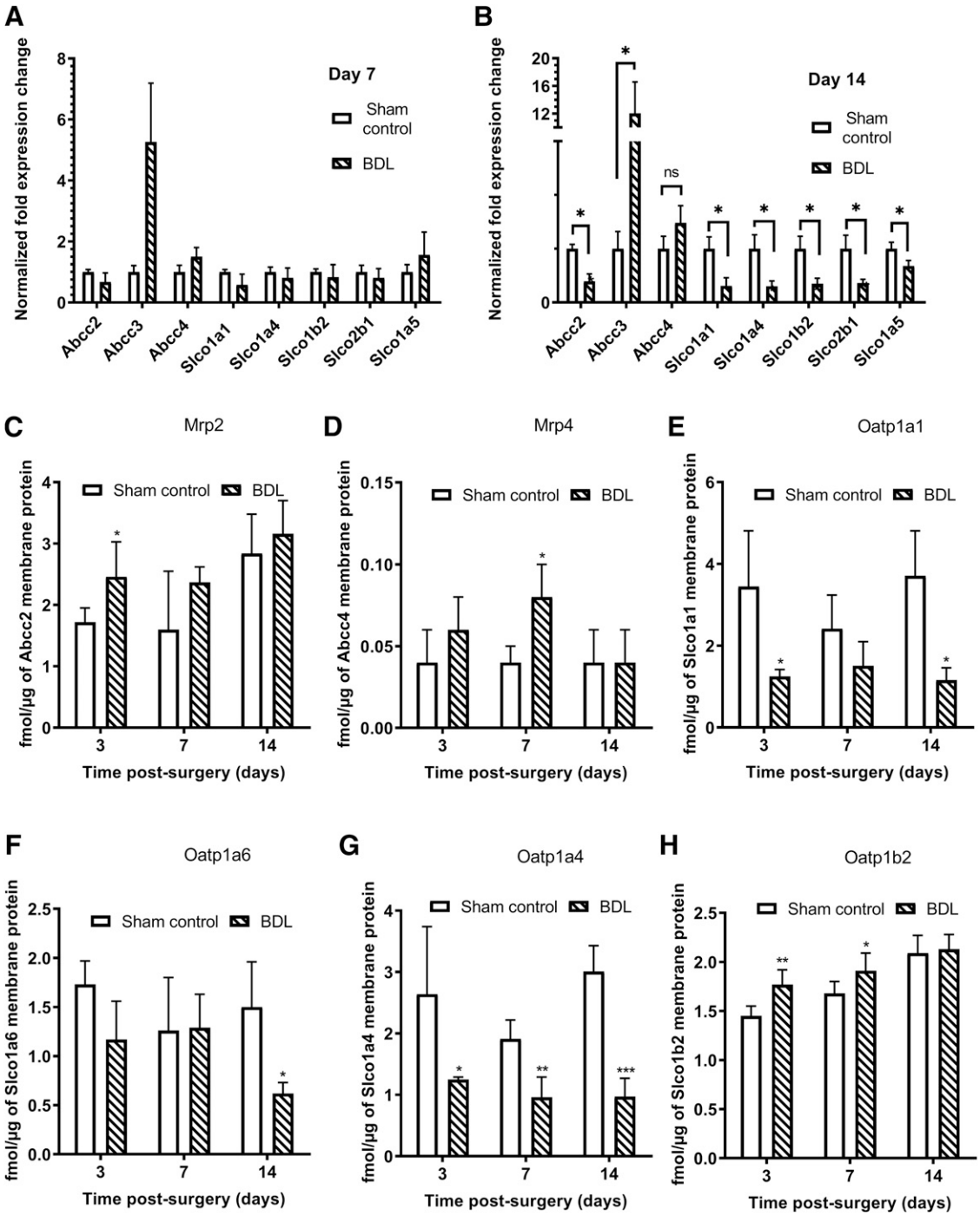

Fig. 3. Transcriptomic and proteomic analysis of hepatic transporters in rat BDL model of fibrosis. (A and B) qPCR-based mRNA estimation of Abcc2, Abcc3, Abcc4, slco1a1, 1a4, 1b2, 2b1, and 1a5 genes from day 7 to day 14 liver samples (n = 4) obtained from the rat BDL study. *$P < 0.05$; **$P < 0.01$; ***$P < 0.001$. (C–H) Proteomics analysis of hepatic transporters in rat BDL study. LC-MS/MS–based protein quantification of day 7 and day 14 liver samples from the rat BDL study conducted for Mrp2,4, Oatp1a1,1a4, 1a6, and 1b2 proteins. *$P < 0.05$; **$P < 0.01$; ***$P < 0.001$.

steatotic livers (n = 20), and NASH livers (n = 19) in a cross-sectional study that included anthropomorphic, liver function, pathology, and liver lipid profile data. MRP4 (*ABCC4*) showed a significant trend of increase compared with healthy control samples or steatotic liver biopsies ($P < 0.001$ and $P < 0.01$, respectively) (Fig. 1A). In addition, upregulation of MRP3 and OATP1B1 expression was also observed ($P < 0.05$ and $P < 0.08$, respectively). We also mapped clinical covariates to the expression profiles of these genes (Fig. 1B). These results suggest that MRP4 and possibly MRP3 and OATP1B1 are associated with NASH in humans.

CP I and III are Substrates of MRP4. As a prelude to further evaluate MRP3 and MRP4 function, we assessed CP I and III as substrates of these transporters. Both CP I and CP III were found to be substrates of MRP3 and MRP4 under the conditions employed in these studies. Uptake of CP I and CP III in MRP3 and MRP4 vesicles was inhibited by the known inhibitors MK-571 and BNZ (Fig. 2). The ratio of uptake in the

TABLE 1

Optimized mass transitions for the labeled and unlabeled peptides for the rat liver transporter quantitation

The peptides represented in italic are the labeled peptides. Q1: parent ion, Q3: product ions, DP: declustering potential, CE: collision energy, NaKATPase: sodium-potassium adenosine triphosphatase.

Protein	Peptide Sequence	Q1	Q3		DP	CE
Mrp2	YFAWEPSFQEQVQGIR	992.9	957.5	473.2	103	44
	YFAWEPSFQEQVQGIR	997.9	967.5	483.2	103	44
Mrp3	TLSDLESNIIAVER	780.4	474.2	901.5	88	37
	TLSDLESNIIAVER	785.4	1040.5	911.5	88	37
Mrp4	APVLFFDR	482.7	796.4	697.3	66	26
	APVLFFDR	487.7	707.3	594.2	66	26
Oatp1a1	GIGETPIVPLGISYIEDFAK	1060.1	480.2	972.4	108	47
	GIGETPIVPLGISYIEDFAK	1064.1	1150.5	980.4	108	47
Oatp1a4	LYLGLPAALR	543.8	810.5	697.4	70	28
	LYLGLPAALR	548.8	820.5	537.3	70	28
Oatp1a6	SENSPFYIGILEVGK	826.9	1235.7	828.5	91	38
	SENSPFYIGILEVGK	830.9	1243.7	723.4	91	38
Oatp1b2	SVQPELK	400.7	614.3	486.2	60	24
	SVQPELK	404.7	622.3	494.3	60	24
NaKATPase	VDNSSLTGESEPQTR	810.3	1004.4	903.4	90	38
	VDNSSLTGESEPQTR	815.3	1014.4	511.2	90	28

presence of ATP to uptake in the presence of AMP in MRP3 vesicles was 25.7 (CP I) and 25.1 (CP III), which decreased to 2.4 and 0.9 (for CP I) and 3 and 2 (for CP III) in the presence of MK-571 and BNZ, respectively. The ATP/AMP uptake ratio of CP I and CP III against MRP4 was 45.3 and 37.7, which decreased to 4.2 and 1.8 (for CP I) and 8.2 and 5.4 (for CP III) in the presence of MK-571 and BNZ, respectively. The affinities (Km) of transport by MRP3 and 4 for both CP I and CP III were found to be similar, 3–6 μM (Supplemental Table 1). Similarly, the Km of CP I in rat MRP4 is also similar to human MRP4, suggesting no significant interspecies difference in affinities.

Hepatobiliary Transporter Expression in Rodent NASH Models. We assessed the hepatobiliary transporter gene and protein expression changes in the rat and mouse BDL NASH models. A significant and gradual increase was observed in the *Abcc*3 gene from day 7 to day 14 in rat BDL livers (Fig. 3, A and B). For the *Slco* transporters, such as *slco1a1*, *1a4, 1b2, 2b1*, and *1a5*, gene expression decreased with time. Similar changes in gene expression were observed for *Abcc3* and the *Slco* family of transporters in MP-treated rat livers (Supplemental File). Significant increase in *Abcc4* was observed in mouse BDL livers compared with sham control. Interestingly, *Slco1a4* increased by 4-fold, whereas *Slco1a1* and *Slco1b2* decreased significantly in BDL mice compared with sham control (Supplemental File).

An LC-MS/MS–based proteomics approach was employed to assess changes in hepatobiliary transporter proteins in rat BDL livers (Table 1). Significant decreases in protein expression of Oatp1a1, 1a4, and 1a6 were observed in BDL livers compared with sham control rat livers on day 14 (Fig. 3, C–H). In contrast, Oatp1b2 protein expression did not change between sham control and rat BDL liver. Mrp3 protein could not be detected in rat livers. Trends to increased Mrp4 expression were observed on day 7 compared with sham control livers, whereas there was no change in Mrp2 protein expression (Fig. 3, C and D).

CP I and III Plasma and Liver Concentrations Increase in the Rat BDL Model. CP I plasma concentration increased 4.5-fold and CP III plasma concentration increased 7-fold on day 14, compared with day 0 plasma concentrations in sham rats (Fig. 4, A and B). As day 0 plasma concentrations provided the highest CP I and III concentrations in sham animals across different days, all comparisons are made with day 0 CP I and III plasma concentrations. The liver CP I and III concentrations (nanograms per gram of liver) increased 1.4–2.8-fold in BDL rats compared with sham-treated rats across different days (Fig. 4, C and D).

CP I and III Plasma and Liver Concentrations Also Increase in Mouse BDL Model. A 40–60-fold increase in plasma concentrations of CP I and III was observed in BDL mice (Fig. 5, A and B) at day 10 postsurgery, compared with sham control. This observation was verified across four independent experiments (data not shown). The liver CP I and III concentrations (nanograms per gram of liver) increased by 9- and 26-fold, respectively, in BDL mice compared with sham-treated mice on day 10 postsurgery (Fig. 5, C and D).

CP I Plasma Concentrations Increase in Alternate Models of NASH in Rats and Mice. To further establish CP I and III as endogenous substrates for hepatobiliary transporters in NASH, we evaluated CP I and III in additional preclinical NASH models in mice and rats. In a dietary model of liver disease in mice, where animals develop chronic disease over several weeks on a choline-deficient high-fat diet (CDAHFD model), the increase in plasma concentrations of CP I is moderate (up to 3-fold), whereas no increase in CP III plasma concentrations was observed (Fig. 6, A and B). The rat MP-induced model provides a path to a longer-term, slower developing, chemically induced, and surgery-independent fibrotic disease that does not involve bile duct ligation but mimics many of its histopathological characteristics. A 4- and 7.5-fold increase in plasma concentrations of CP I and III was observed after 6 weeks of MP treatment, compared with saline-treated rats (Fig. 6, C and D).

Discussion

In the transporter mRNA analysis, we found *ABCC4* (*ABCC* corresponds to MRP protein) to increase significantly in patients with NASH and steatosis compared with healthy subjects. Interestingly, clinical staging of NASH was the single largest covariate with *ABCC*4 expression in the Canadian cohort (Fig. 1B). Other covariates include NASH Clinical Research Network score, body mass index, and diagnosis of liver disease. Of the five transporters evaluated, *ABCC*4 shows the strongest correlation with these parameters. Increased Abcc4 mRNA is also reported in CDAHFD model in

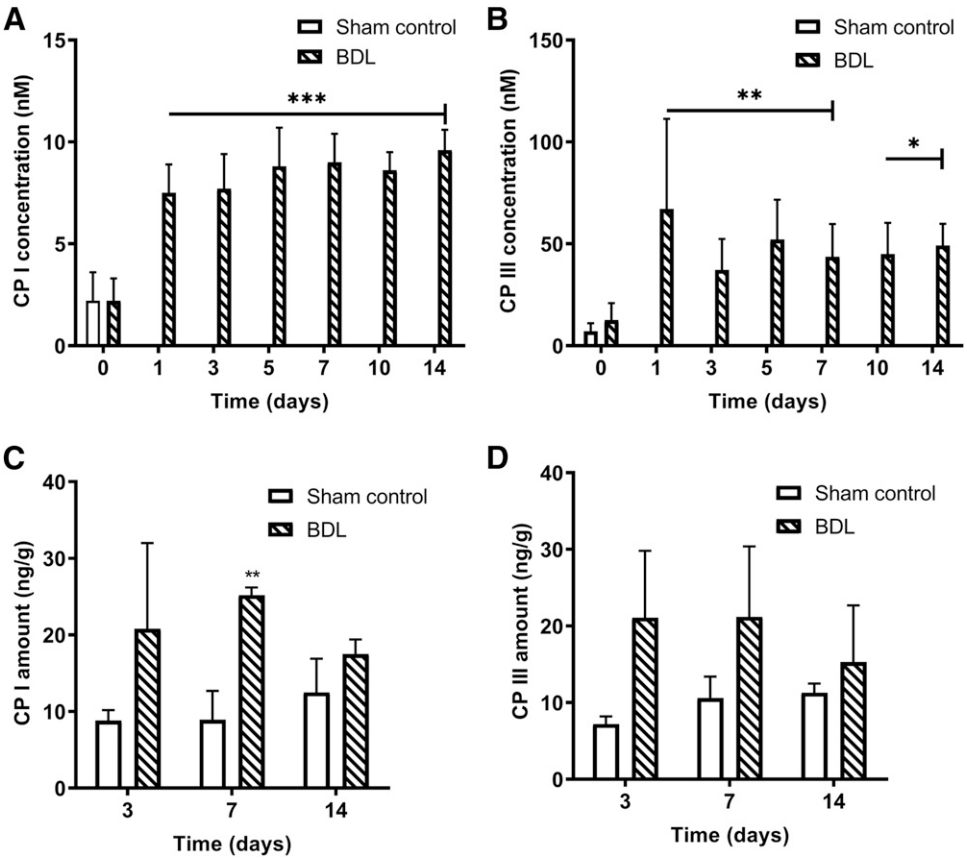

Fig. 4. CP I and III plasma concentration (A and B) and liver accumulation (C and D) in bile duct–ligated Sprague-Dawley rats. Bile duct ligation was conducted on day 1, and samples were taken on day 0 (presurgery, $n = 12$), day 1 ($n = 12$), day 3 ($n = 12$), day 5 ($n = 8$), day 7 ($n = 8$), day 10 ($n = 4$), and day 14 ($n = 4$). Plasma concentrations from BDL rats were compared with day 0 sham control rats ($n = 4$), and liver accumulation was compared with corresponding sham control liver. $^{*}P < 0.05$; $^{**}P < 0.01$; $^{***}P < 0.001$.

mice (Suga et al., 2019). The French-Belgian cohort compared patients with NASH with healthy controls. A 1-year follow-up was performed on a subset of patients ($n = 14$) with interventional treatment to demonstrate clinical stage reversal of disease. In this cohort, *ABCC4* mRNA expression decreased after 1 year of bariatric surgery and dietary restrictions, compared with the same subjects at T0 (initial time of sampling), when they were clinically classified with NASH (Fig. 7). This suggests that transporter expression may be concurrently regulated with disease progression. Therefore, specific endogenous substrates of these transporters could be used as plasma-based biomarkers to track disease progression. There are very few markers that can complement noninvasive imaging or elastographic measurements. Thus, this novel strategy can be a significant value addition to the field.

The changes in mRNA expression of transporters in animal models are more pronounced than in humans, with *Abcc3* increasing 10–15-fold in both rat BDL and MP-induced rat models of fibrosis. A statistically nonsignificant trend to increased *Abcc4* was also observed. *Slco* transporter gene expression decreased 3–4-fold in both animal models. Interestingly, mouse BDL livers showed significant increase in *Abcc4* gene. Maximum increase of CP I and III plasma concentrations was also observed in mouse BDL compared with sham control, suggesting possible correlation of CP I and III plasma concentrations with *Abcc4* gene (Mrp4 protein) expression.

Unlike gene expression, protein expression of Oatp1b2 remains constant in the BDL rat livers until day 14. Oatp1a1, 1a4, and 1a6 protein expressions decreased at day 14 in BDL rat livers (Fig. 3, C–H). Mrp3 protein could not be quantitated in the rat BDL model because of the low expression level of Mrp3 in rats. The protein expression level of Mrp3 is lowest in rats compared with human, monkey, and dog (Wang et al., 2015). Therefore, the increased mRNA of *Abcc3* could not be corroborated with protein expression. The disconnect between gene and protein level changes reinforces the need for functional activity information about the OATP-MRP axis transporters.

CP I and III are endogenous compounds reported to be substrates of OATP1B, MRP2, and MRP3 transporters (Lai et al., 2016; Shen et al., 2016; Gilibili et al., 2017; Kunze et al., 2018). Plasma and urinary CP I and III have previously been used as biomarkers of OATP1B and MRP2 transporter function in vivo (Kondo et al., 1976; Wolkoff et al., 1976; Benz-de Bretagne et al., 2014; Lai et al., 2016). To complete the OATP-MRP axis of transporters, we evaluated CP I and III as substrates for MRP4. Additionally, the significant association of MRP4 with disease progression highlighted the importance of investigating any potential MRP4 probe substrate. A previous study (Kunze et al., 2018) did not find a sufficient signal for CP I and III against MRP4 in a vesicle assay. However, our studies demonstrate a significant signal to noise ratio for CP I and III against both MRP3 and 4. Differences in study design, for example, detection method (fluorescence vs. radioactivity), vesicle source (HEK cells from PharmTox vs. Sf9 from Genomembrane), or final eluant (methanol vs. sodium dodecyl sulfate 0.5% in water) may have contributed to the differences between Kunze et al. and our study. This is the first report showing CPI and III as substrates of

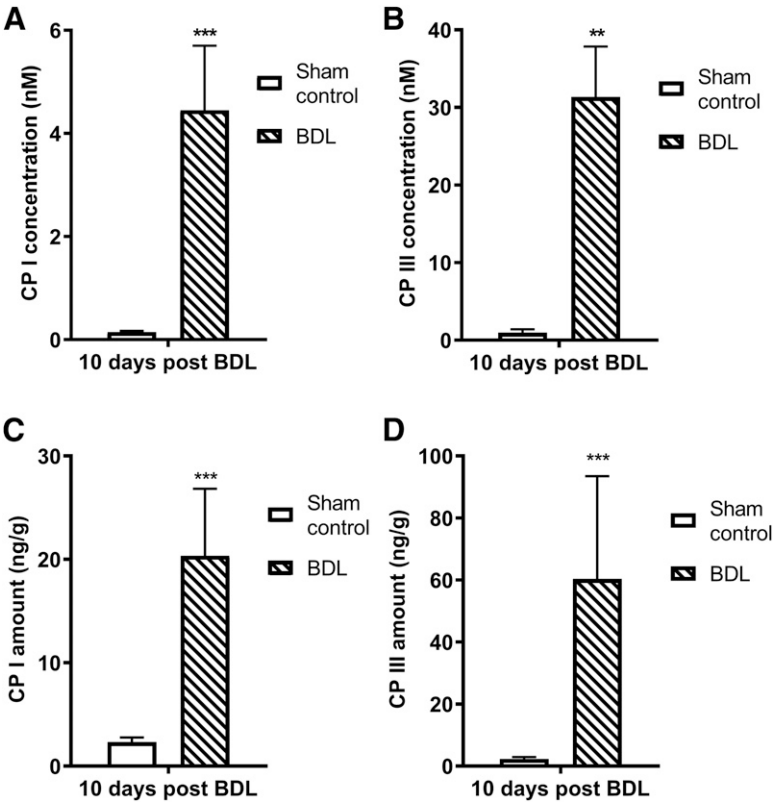

Fig. 5. CP I and III plasma concentration (A and B) and liver accumulation (C and D) in bile duct–ligated C57BL/6 mice. Bile duct ligation was conducted on day 3, and samples were taken on day 10 at the end of the study. Plasma concentrations from BDL mice (n = 12) were compared with day 10 sham control rats (n = 6), and liver accumulation in BDL mice was compared with corresponding sham control liver. $^{**}P < 0.01$; $^{***}P < 0.001$.

MRP4. Therefore, plasma concentrations of CP I and III become potential candidates to understand NASH-related changes in the OATP-MRP axis of transporters.

The expression and functional changes in OATP-MRP axis of transporters, namely, 1) decreased OATP-mediated uptake, 2) increased MRP3/4-mediated basolateral efflux, or

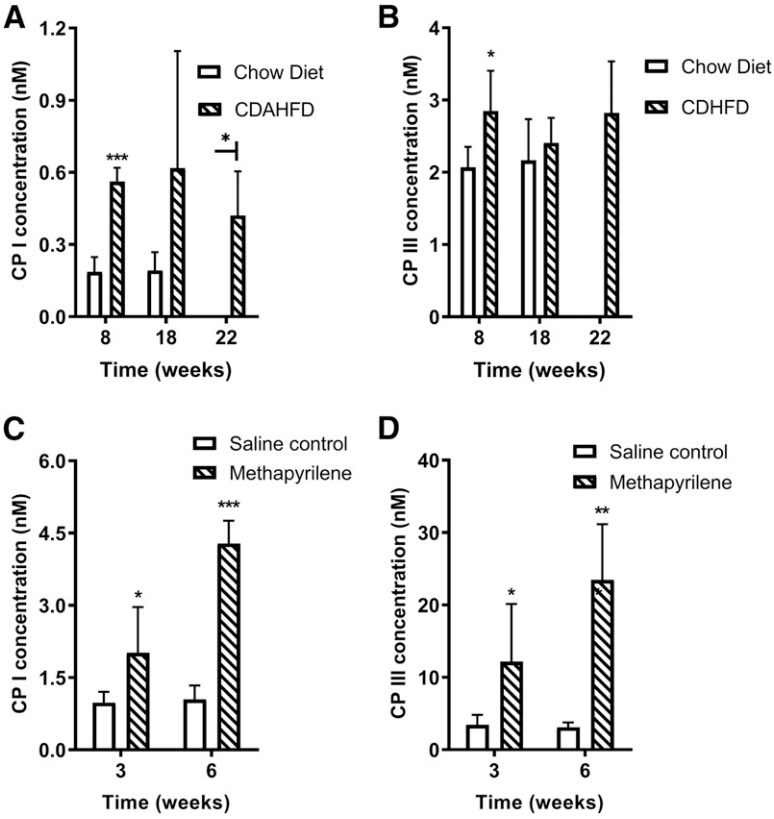

Fig. 6. CP I and CP III concentrations in other preclinical models across species. (A and B) CP I and III plasma concentration in choline-deficient high-fat diet–fed mice. At 7 weeks of age, mice were placed on either a matched normal chow diet containing standard levels of choline, methionine, and fat (A13012807; Research Diets) or were placed on a choline-deficient amino acid–defined (methionine 0.1%), high-fat (60% of calories from fat) diet, CDAHFD. Plasma samples were collected from each animal (n = 5 at each time point) at 8, 18, or 22 weeks. (C and D) CP I and III plasma concentration in methapyrilene-induced Sprague-Dawley rat model of NASH. Plasma CP concentrations from PBS-dosed rats (n = 5, each of 3 and 6 weeks) were compared with plasma concentrations from 150 mg/kg methapyrilene-treated rats (po, thrice weekly). Number of rats from treatment group are 5 and 4, for third and sixth week of treatment, respectively. $^{*}P < 0.05$; $^{**}P < 0.01$; $^{***}P < 0.001$.

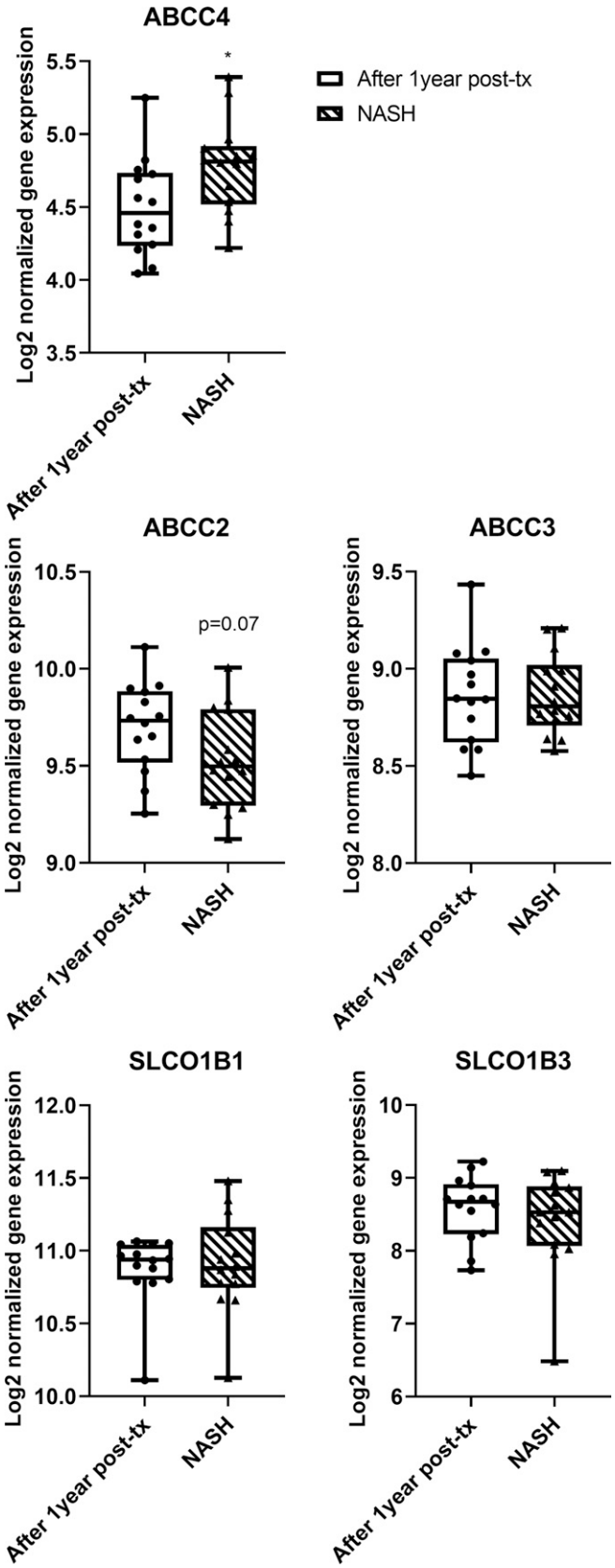

Fig. 7. Transporter gene expression in patients with clinical stage reduction in disease. The French-Belgian cohort established gene expression profiles in a large cross-sectional study. The subset depicted herein tracked 14 patients with NASH after 1 year of interventional therapy (post-tx), with clinical stage reduction in disease. The French-Belgian cohort was profiled for global gene expression using GeneChip Human Gene 2.0 ST Array, as documented with GEO identifier GSE83452.

3) mislocalization of MRP2, can lead to increased plasma and liver concentrations of drugs and endogenous compounds. To evaluate if CP I and III follow the transporter changes observed in NASH, plasma and liver concentrations in various NASH rodent models were assessed. To our knowledge, this is the first report of plasma and liver concentrations of CP I and III compared across different preclinical models of NASH. There is no single animal model that completely mimics human NASH pathophysiology. Therefore, we assessed the plasma concentration of CP I and III in 1) surgical NASH models, both rat and mouse BDL where cholestatic disease is observed (mouse BDL is accompanied by gall bladder dilation). Cholestatic liver injury is a major cause of liver fibrosis and cirrhosis in patients with either acute or chronic liver disease; 2) MP-induced fibrosis in rat, a chemical-induced NASH to mimic bile duct ligation in a more chronic mode; and 3) in a mouse diet-induced NASH model CDAHFD). This is a chronic model that factors in steatosis, a hallmark of human disease. However, the metabolic profile of this model does not completely reflect all properties of NASH in humans (reviewed by Liedtke et al., 2013 and Liu et al., 2013).

We have previously optimized all these models to demonstrate fibrosis at the time points studied, as evidenced by hydroxyproline levels and histopathological evaluation (e.g., both rat and mouse BDL models show portal and bridging fibrosis without cirrhosis at day 14 and day 10, respectively). In all models, significant increase in CP I plasma concentration was observed, whereas CP III plasma concentration increased in all but the CDAHFD model. Diet-induced models have been suggested to reflect human relevant transporter changes (Li et al., 2018). Hence, CP I may be more sensitive than CP III as a marker of transporter activity changes. Across different models and modes of NASH induction, the observed increase in CP plasma concentration suggests that they can be used as endogenous plasma-based biomarkers, especially in conjunction with other small molecules, such as bile acids (Puri et al., 2018; Luo et al., 2019).

The increase in liver concentrations of CP I and III are consistent with previous reports with MEB (Ali et al., 2017). Similar to rat BDL, in mouse BDL experiments, CP I and III hepatic concentrations also increased significantly (Figs. 4 and 5). Although we have not evaluated Mrp2 internalization in this work, this phenomenon is heavily reported in NASH and cholestasis models, including rat BDL (Paulusma et al., 2000). Previous reports demonstrated a 60% reduction in biliary elimination in pemetrexed (Mrp2 substrate) in the diet-induced NASH model without any statistically significant change in mRNA of protein expression (Dzierlenga et al., 2016). Mrp2 internalization will have a significant impact on hepatic concentrations of compounds. The hepatic concentration changes can impact efficacy of the compounds directly if the intended target is in liver. In addition, for compounds where the mechanism of toxicity is linked to liver targets (e.g., drug-induced cholestasis), increased hepatic concentrations can potentiate safety risks. Hence, changes in hepatic concentrations of drugs become critical because of possible effects on safety and efficacy. For understanding a direct role of MRP/Mrp2, 3, or 4 in plasma CP concentration changes during NASH, disease can be induced in individual transporter knockout preclinical models. A complicating factor in the specificity of plasma CPs as NASH biomarkers could be the impact of NASH on the synthesis of CPs in erythrocytes

and in liver. Although no reports were identified, the scope of this study cannot exclude such a complication. Future work using a labeled precursor of CP biosynthesis may address the effects of NASH on CP biosynthesis.

There are different approaches to qualitatively or quantitatively assess the impact of transporter alterations in NASH. Repeated liver biopsy on the same subject is challenging in a clinical setting. In addition, translating mRNA expression to functional activity can be difficult. Another potential method to assess transporter activity changes is to evaluate the pharmacokinetics of a probe compound (which is a substrate of the relevant transporters) in a patient population. Ali et al. employed the nuclear imaging agent ^{99m}Tc-MEB in patients with NASH to quantitate compound disposition (Ali et al., 2017). However, MEB is not a sensitive substrate of MRP3, as basolateral efflux is stimulated rather than inhibited by the MRP3 inhibitor MK-571 (Swift et al., 2010). In another recent approach, a physiologically based pharmacokinetic (PBPK) model based on transporter proteomics data from NASH and steatotic liver samples was used (Vildehede et al., 2020). However, the protein expression–based PBPK model was unable to capture the liver accumulation of MEB. The model required a 5-fold decrease in MRP2 activity that could not be attributed to the protein expression changes alone. This highlights some key drawbacks of proteomics-based PBPK to predict transporter activity changes. An endogenous compound with plasma concentrations that are sensitive to transporter functional changes can overcome the challenges to assess the impact of NASH on transporters—an important aspect as new therapies for the disease enter clinical trials. Tracking CP I/III plasma concentrations in patients can facilitate dose adjustment strategies for transporter substrates used or to be used in NASH treatments. To further evaluate CP I and III as potential plasma-based biomarkers in NASH, the following experiments can be carried out: 1) evaluation of the effect of drug treatment in preclinical models on plasma concentrations of CP I/III, 2) evaluation of the effect of disease and clinical stage reduction in human plasma with concentrations of CP I and III, and 3) evaluation of the association of CP I and III with other histologic/imaging-based markers of NASH.

In summary, liver transporters MRP4, MRP3, and OATP1B1 are altered in patients with clinically staged fatty liver disease and NASH. These changes are also observed in various preclinical models of NASH in rodents. In addition, we have shown that CP I and III are substrates of the transporters of the OATP-MRP axis. Altered expression of OATP-MRP transporters can also be correlated with the pharmacokinetic changes of CP I and CP III observed in preclinical NASH models. Taken together, these results suggest that liver transporters are modified in patients with NASH, which may impact the disposition of endo- and xenobiotics. In addition, this study provides experimental evidence that CP I and III can be used as potential plasma-based biomarkers of NASH progression.

Acknowledgments

The authors thank Anup Deshpande, Ram Vishwanath, Manoj Verma, Vijay Marshal, Rajeev Kumar, Erica Toth, Punit Marathe, Sabariya Selvam, and Stephanie Boehm for help during various aspects of this work, such as data analysis, experimental setup, and reviewing the manuscript.

Authorship Contributions

Participated in research design: Chatterjee, Mukherjee, Shen.

Conducted experiments: Sankara Sivaprasad, Naik, Gautam, Murali, Hadambar, Gunti, Basavanthappa, Zinker, Zhang.

Contributed new reagents or analytical tools: Chatterjee, Mukherjee, Mariappan, Ramarao, Sinz, Shen.

Performed data analysis: Chatterjee, Mukherjee, Sankara Sivaprasad, Naik, Murali, Kuchibotla, Deyati, Mariappan, Zinker, Shen.

Wrote or contributed to the writing of the manuscript: Chatterjee, Mukherjee, Sinz, Shen.

References

Ali I, Slizgi JR, Kaullen JD, Ivanovic M, Niemi M, Stewart PW, Barritt AS IV, and Brouwer KLR (2017) Transporter-mediated alterations in patients with NASH increase systemic and hepatic exposure to an OATP and MRP2 substrate. *Clin Pharmacol Ther* **104**:749–756.

Benz-de Bretagne I, Zahr N, Le Gouge A, Hulot JS, Houillier C, Hoang-Xuan K, Gyan E, Lissandre S, Choquet S, and Le Guellec C (2014) Urinary coproporphyrin I/(I + III) ratio as a surrogate for MRP2 or other transporter activities involved in methotrexate clearance. *Br J Clin Pharmacol* **78**:329–342.

Brunt EM, Wong VWS, Nobili V, Day CP, Sookoian S, Maher JJ, Bugianesi E, Sirlin CB, Neuschwander-Tetri BA, and Rinella ME (2015) Nonalcoholic fatty liver disease. *Nat Rev Dis Primers* **1**:15080.

Chalasani N, Younossi Z, Lavine JE, Charlton M, Cusi K, Rinella M, Harrison SA, Brunt EM, and Sanyal AJ (2018) The diagnosis and management of nonalcoholic fatty liver disease: practice guidance from the American Association for the Study of Liver Diseases. *Hepatology* **67**:328–357.

Cobbina E and Akhlaghi F (2017) Non-alcoholic fatty liver disease (NAFLD) - pathogenesis, classification, and effect on drug metabolizing enzymes and transporters. *Drug Metab Rev* **49**:197–211.

Clarke JD, Dzierlenga AL, Nelson NR, Li H, Werts S, Goedken MJ, and Cherrington NJ (2015) Mechanism of altered metformin distribution in nonalcoholic steatohepatitis. *Diabetes* **64**:3305–3313.

Clarke JD, Hardwick RN, Lake AD, Canet MJ, and Cherrington NJ (2014a) Experimental nonalcoholic steatohepatitis increases exposure to simvastatin hydroxy acid by decreasing hepatic organic anion transporting polypeptide expression. *J Pharmacol Exp Ther* **348**:452–458.

Clarke JD, Hardwick RN, Lake AD, Lickteig AJ, Goedken MJ, Klaassen CD, and Cherrington NJ (2014b) Synergistic interaction between genetics and disease on pravastatin disposition. *J Hepatol* **61**:139–147.

Clarke JD, Novak P, Lake AD, Hardwick RN, and Cherrington NJ (2017) Impaired N-linked glycosylation of uptake and efflux transporters in human non-alcoholic fatty liver disease. *Liver Int* **37**:1074–1081.

Dzierlenga AL, Clarke JD, Hargraves TL, Ainslie GR, Vanderah TW, Paine MF, and Cherrington NJ (2015) Mechanistic basis of altered morphine disposition in nonalcoholic steatohepatitis. *J Pharmacol Exp Ther* **352**:462–470.

Dzierlenga AL, Clarke JD, Klein DM, Anumol T, Snyder SA, Li H, and Cherrington NJ (2016) Biliary elimination of Pemetrexed is dependent on Mrp2 in rats: potential mechanism of variable response in nonalcoholic steatohepatitis. *J Pharmacol Exp Ther* **358**:246–253.

Evers R, Piquette-Miller M, Polli JW, Russel FGM, Sprowl JA, Tohyama K, Ware JA, de Wildt SN, Xie W, and Brouwer KLR; International Transporter Consortium (2018) Disease-associated changes in drug transporters may impact the pharmacokinetics and/or toxicity of drugs: a white paper from the international transporter consortium. *Clin Pharmacol Ther* **104**:900–915.

Gautam SS, Wagh S, Babu S, Gudihal R, Rajagopalan S, Kole P, Mandlekar S, and Subramanian M (2019) Relative quantitation of endogenous proteins by quadrupole-time of flight and tandem mass spectrometry. *J Chromatogr B Analyt Technol Biomed Life Sci* **1106–1107**:11–18.

Gilibili RR, Chatterjee S, Bagul P, Mosure KW, Murali BV, Mariappan TT, Mandlekar S, and Lai Y (2017) Coproporphyrin-I: a fluorescent, endogenous optimal probe substrate for ABCC2 (MRP2) suitable for vesicle-based MRP2 inhibition assay. *Drug Metab Dispos* **45**:604–611.

Hardwick RN, Clarke JD, Lake AD, Canet MJ, Anumol T, Street SM, Merrell MD, Goedken MJ, Snyder SA, and Cherrington NJ (2014) Increased susceptibility to methotrexate-induced toxicity in nonalcoholic steatohepatitis. *Toxicol Sci* **142**: 45–55.

Kondo T, Kuchiba K, and Shimizu Y (1976) Coproporphyrin isomers in Dubin-Johnson syndrome. *Gastroenterology* **70**:1117–1120.

Kunze A, Ediage EN, Dillen L, Monshouwer M, and Snoeys J (2018) Clinical investigation of coproporphyrins as sensitive biomarkers to predict mild to strong OATP1B-mediated drug–drug interactions. *Clin Pharmacokinet* **57**:1559–1570.

Laho T, Clarke JD, Dzierlenga AL, Li H, Klein DM, Goedken M, Micuda S, and Cherrington NJ (2016) Effect of nonalcoholic steatohepatitis on renal filtration and secretion of adefovir. *Biochem Pharmacol* **115**:144–151.

Lai Y, Mandlekar S, Shen H, Holenasipur VK, Langish R, Rajanna P, Murugeshan S, Gaud N, Selvam S, Date O, et al. (2016) Coproporphyrins in plasma and urine can be appropriate clinical biomarkers to recapitulate drug-drug interactions mediated by organic anion transporting polypeptide inhibition. *J Pharmacol Exp Ther* **358**:397–404.

Li H, Toth E, and Cherrington NJ (2018) Asking the right questions with animal models: methionine- and choline-deficient model in predicting adverse drug reactions in human NASH. *Toxicol Sci* **161**:23–33.

Lickteig AJ, Fisher CD, Augustine LM, Aleksunes LM, Besselsen DG, Slitt AL, Manautou JE, and Cherrington NJ (2007) Efflux transporter expression and acetaminophen metabolite excretion are altered in rodent models of nonalcoholic fatty liver disease. *Drug Metab Dispos* **35**:1970–1978.

Liedtke C, Luedde T, Sauerbruch T, Scholten D, Streetz K, Tacke F, Tolba R, Trautwein C, Trebicka J, and Weiskirchen R (2013) Experimental liver fibrosis research: update on animal models, legal issues and translational aspects. *Fibrogenesis Tissue Repair* **6**:19–43.

Lin CH and Kohli R (2018) Bile acid metabolism and signaling: potential therapeutic target for nonalcoholic fatty liver disease. *Clin Transl Gastroenterol* **9**:164.

Liu Y, Meyer C, Xu C, Weng H, Hellerbrand C, ten Dijke P, and Dooley S (2013) Animal models of chronic liver diseases. *Am J Physiol Gastrointest Liver Physiol* **304**:G449–G468.

Luo Y, Charles ED, Shipkova P, Reily M, Jarai G, and Sanyal A (2019) Pegbelfermin (BMS-986036) reduces serum levels of secondary bile acids in patient with non-alcoholic steatohepatitis. The International Liver Congress 2019: Annual Meeting of the European Association for the Study of the Liver, Vienna, Austria, FRI-323.

Paulusma CC, Kothe MJ, Bakker CTM, Bosma PJ, van Bokhoven I, van Marle J, Bolder U, Tytgat GNJ, and Oude Elferink RPJ (2000) Zonal down-regulation and redistribution of the multidrug resistance protein 2 during bile duct ligation in rat liver. *Hepatology* **31**:684–693.

Probert PM, Ebrahimkhani MR, Oakley F, Mann J, Burt AD, Mann AD, and Wright MC (2014) A reversible model for periportal fibrosis and a refined alternative to bile duct ligation. *Toxicol Res* **3**:98–109.

Puri P, Daita K, Joyce A, Mirshahi F, Santhekadur PK, Cazanave S, Luketic VA, Siddiqui MS, Boyett S, Min HK, et al. (2018) The presence and severity of non-alcoholic steatohepatitis is associated with specific changes in circulating bile acids. *Hepatology* **67**:534–548.

Shen H, Dai J, Liu T, Cheng Y, Chen W, Freeden C, Zhang Y, Humphreys WG, Marathe P, and Lai Y (2016) Coproporphyrins I and III as functional markers of OATP1B activity: in vitro and in vivo evaluation in preclinical species. *J Pharmacol Exp Ther* **357**:382–393.

Suga T, Yamaguchi H, Ogura J, Shoji S, Maekawa M, and Mano N (2019) Altered bile acid composition and disposition in a mouse model of non-alcoholic steatohepatitis. *Toxicol Appl Pharmacol* **379**:114664.

Sun J, Ahmad S, Chen S, Tang W, Zhang Y, Chen P, and Lin X (2005) Cochlear gap junctions coassembled from Cx26 and 30 show faster intercellular Ca2+ signaling than homomeric counterparts. *Am J Physiol Cell Physiol* **288**:C613–C623.

Suzuki Y, Ono H, Tanaka R, Sato F, Sato Y, Ohno K, Mimata H, and Itoh H (2019) Recovery of OATP1B activity after living kidney transplantation in patients with end-stage renal disease. *Pharm Res* **36**:59.

Swift B, Yue W, and Brouwer KL (2010) Evaluation of (^{99m})technetium-mebrofenin and (^{99m})technetium-sestamibi as specific probes for hepatic transport protein function in rat and human hepatocytes. *Pharm Res* **27**:1987–1998.

Tag CG, Sauer-Lehnen S, Weiskirchen S, Borkham-Kamphorst E, Tolba RH, Tacke F, and Weiskirchen R (2015) Bile duct ligation in mice: induction of inflammatory liver injury and fibrosis by obstructive cholestasis. *J Vis Exp* **96**:52438.

Takita M, Ikawa S, and Ogura Y (1988) Effect of bile duct ligation on bile acid and cholesterol metabolism in rats. *J Biochem* **103**:778–786.

Thakkar N, Slizgi JR, and Brouwer KLR (2017) Effect of liver disease on hepatic transporter expression and function. *J Pharm Sci* **106**:2282–2294.

Wang B, Rudnick S, Cengia B, and Bonkovsky HL (2018) Acute hepatic porphyrias: review and recent progress. *Hepatol Commun* **3**:193–206.

Wang L, Prasad B, Salphati L, Chu X, Gupta A, Hop CE, Evers R, and Unadkat JD (2015) Interspecies variability in expression of hepatobiliary transporters across human, dog, monkey, and rat as determined by quantitative proteomics. *Drug Metab Dispos* **43**:367–374.

Wolkoff AW, Wolpert E, Pascasio FN, and Arias IM (1976) Rotor's syndrome. A distinct inheritable pathophysiologic entity. *Am J Med* **60**:173–179.

Vildhede A, Kimoto E, Pelis RM, Rodrigues AD, and Varma MVS (2020) Quantitative proteomics and mechanistic modeling of transporter-mediated disposition in non-alcoholic fatty liver disease. *Clin Pharmacol Ther* **107**:1128–1137.

Yang Y, Chen B, Chen Y, Zu B, Yi B, and Lu K (2015) A comparison of two common bile duct ligation methods to establish hepatopulmonary syndrome animal models. *Lab Anim* **49**:71–79.

Address correspondence to: Sagnik Chatterjee, Pharmaceutical Candidate Optimization, Biocon Bristol-Myers Squibb R&D Center (BBRC), Syngene International Ltd., Jigani Link Rd., Bangalore 560099, India. E-mail: sagnik.chatterjee@syngeneintl.com

Article title: Transporter activity changes in non-alcoholic steatohepatitis: assessment with plasma coproporphyrin I and III

Authors: Sagnik Chatterjee[*§], Sambuddho Mukherjee[*], Sankara Sivaprasad LVJ, Tanvi Naik, Shashyendra Singh Gautam, Bokka Venkata Murali, Avinash Annasao Hadambar, Gowtham Raj Gunti, Vijaykumar Kuchibotla, Avisek Deyati, Sushma Basavanthappa, Manjunath Ramarao, T. Thanga Mariappan, Bradley A. Zinker, Yueping Zhang, Michael Sinz, Hong Shen

Journal title: Journal of Experimental Pharmacology and Therapeutics (JPET)

Manuscript number: JPET-AR-2020-000291

Supplementary information S1: Rat Transporter Protein quantitation:

Membrane protein isolation:

Liver (200 mg) from both sham and BDL rats were subjected to membrane fraction isolation procedure using the ProteoExtract Native Membrane Protein Extraction Kit from Calbiochem (CA, USA), as per manufacturer's protocol. Briefly, the tissues were washed twice in ice-cold wash buffer and then the tissue samples were homogenized with a Dounce tissue grinder (Fisher Scientific, Tustin, CA) with 2mL of extraction buffer-I and then incubated for 10 min at 4°C. Protease inhibitor cocktail (PIC; 10 µL) was added to prevent any proteases activity which gets released from the cells. The homogenate is then centrifuged at 16000g for 20 minutes, the pellet thus obtained was then incubated with 1 ml of ice-cold extraction buffer II supplemented with 5µL PIC for 30 min at 4°C under gentle agitation. The cell suspension was centrifuged at 16,000 g for 15 min at 4°C and the supernatant containing membrane proteins was collected. Protein concentrations were measured using the Bicinchoninic acid protein assay kit from Pierce (Rockford, IL, USA), manufacturer's protocol was followed for protein estimation and the bovine serum albumin was used to make calibration curves.

Instrumentation and chromatographic procedural details:

The Waters Acquity UPLC (ultra-performance liquid chromatography) Integrated System was run in gradient mode at a flow rate of 0.4 mL/min with mobile phase A containing 0.1% formic acid in water and mobile phase B with 0.1% formic acid in acetonitrile with a run time of 4.2 min. Quantitation was achieved by MS/MS detection in positive ion, multiple reaction

monitoring (MRM) mode, for selected peptides using API 5500 mass spectrometer (Applied Biosystems, MDS Sciex Toronto, Canada) equipped with an API electrospray ionization (ESI) source.

Trypsin digestion procedure:

To determine the sensitive peptides for individual transporters and their expression levels, an efficient and simple digestion method was adopted. The membrane fraction (500 µg) was mixed with 150 µL of methanol, the sample was centrifuged at 2000 xg, the supernatant was discarded and the pellet was air-dried. The pellet was resuspended using 100 µl of 100 mM ammonium bicarbonate (AMBIC) along with 50 µL of 3.5 % of sodium deoxycholate (DOC) and was subjected to heat denaturation for 30 min at 80°C. DTT (dithiothreitol) (20 µL of 200 mM) was added to the mixture and kept in thermo mixture at 700 rpm at 60 °C for 20 min. IAM (Iodoacetamide) (20 µl of 100 mM) was added to the mixture and kept in the dark for 1 hr. Sequence grade trypsin was added at a 1:10 ratio and the samples were incubated overnight at 37 °C. The digested protein solution was terminated by adding an appropriate amount of 10% v/v formic acid in water. Samples were subsequently vortexed, centrifuged, the supernatant dried and then reconstituted with 0.1 % formic acid in water prior to LC-MS/MS analysis.

Selection of unique peptides:

Briefly, the observed peptides from each rat transporter protein Mrp2, Mrp3, Mrp4, Oatp1a1, Oatp1a4, Oatp1a6, Oatp1b2, and Ostβ were checked for its reproducibility and repeatability (n=3). Each identified peptide was then searched using BLAST (Basic local alignment search tool), provided by NCBI (National Centre for Biotechnology Information) against the rat non-redundant database. Each peptide was selected based on their identity, peptides with an identity of 100% were progressed for further screening of the E-value (E-value is the number of expected hits of similar quality that could be found just by chance) where each peptides has to pass an E-value cut-off of less than 0.01. There were instances when more than one peptide satisfied the criteria, and for this kind of scenario, the peptides which showed no interference in the blank samples and better MS signal were given preference. Additionally, other criteria relevant to MS detection of peptides as previously described were also applied[1].

Reference

1) Liebler, C.D., and Zimmerman, L.J. Targeted Quantitation of Proteins by Mass Spectrometry. *Biochemistry*. **52**, 3797–3806 (2013).

Supplementary Table 1

Transport kinetics of coproporphyrin I (CP I) and coproporphyrin III (CP III) in human MRP3, 4, and rat Mrp4 overexpressed membrane vesicles. Graphpad Prism is used to calculate kinetic constants (Vmax and Km). Values from two independent experiments are listed for MRP3 and 4, while for rat Mrp4 one experiment is conducted. Each experiment was conducted in triplicate wells. Standard Error (SE) is calculated in Graphpad Prism.

Compound	MRP3		MRP4		rMrp4	
	Km ± S.E (µM)	Vmax ± S.E (pmol/min/mg)	Km ± S.E (µM)	Vmax ± S.E (pmol/min/mg)	Km ± S.E (µM)	Vmax ± S.E (pmol/min/mg)
CP I	4.3 ± 0.5 , 3.2 ± 0.2	489 ± 16.2, 338 ± 6.5	5.3 ± 0.4, 5.7 ± 0.3	308.5 ± 7.9, 277.1 ± 4.6	4.8 ± 0.6	257.9 ± 7.4
CP III	3 ± 0.3	116 ± 16.9	2.5 ± 0.3	363.7 ± 2.5		

Supplementary Figure 1: Transporter transcriptomics in mouse BDL model

Supplementary figure

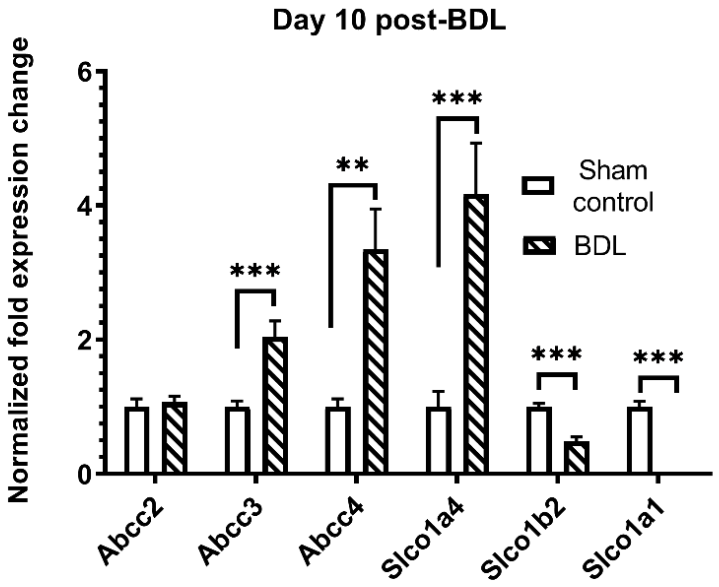

Supplemental Figure 1: qPCR based mRNA estimation of *Abcc2, Abcc3, Abcc4, slco1a4, 1b2*, and *1a1* genes from day-10 sham and mouse BDL liver samples obtained from the mouse BDL study. *: $p < 0.05$, **: $p < 0.01$, ***: $p < 0.001$.

Supplementary Figure 2: Transporter transcriptomics in mouse BDL model

Supplementary figure

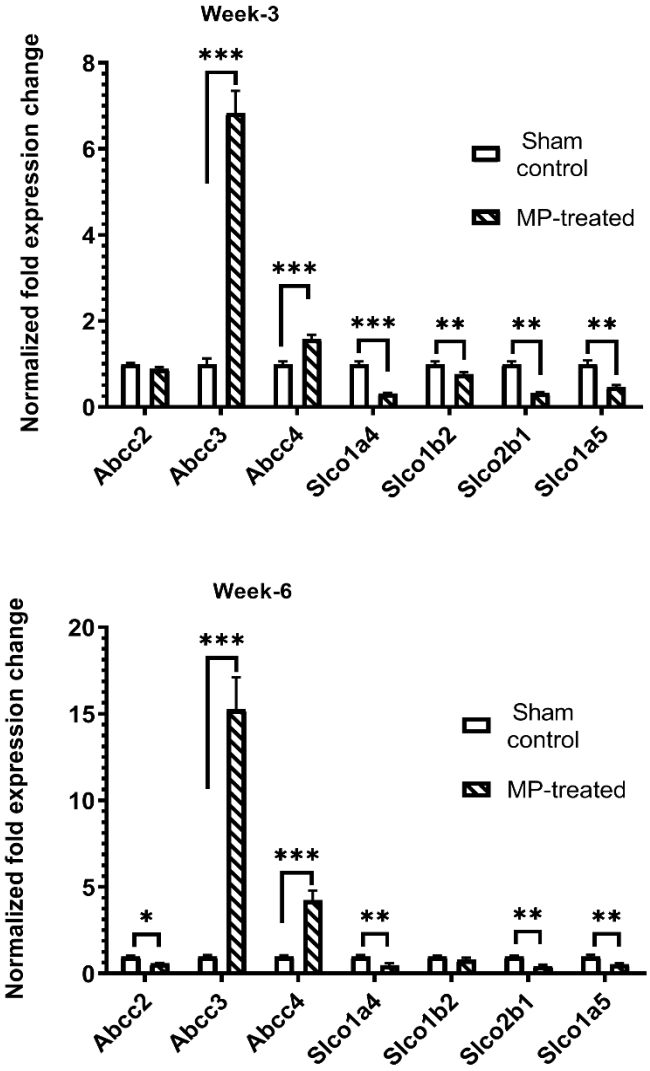

Supplemental Figure 2: qPCR based mRNA estimation of *Abcc2, Abcc3, Abcc4, slco1a4, 1b2,* i, and *1a5* genes from 3 weeks and 6 weeks' saline treated and MP-treated rat liver samples obtained from the rat MP-induced NASH study. *: $p < 0.05$, **: $p < 0.01$, ***: $p < 0.001$.